



Evaluating the energy consumption of electric vehicles based on car-following model under non-lane discipline

Yongfu Li · Li Zhang · Hong Zheng ·
Xiaozheng He · Srinivas Peeta ·
Taixiong Zheng · Yinguo Li

Received: 17 December 2014 / Accepted: 23 May 2015 / Published online: 9 June 2015
© Springer Science+Business Media Dordrecht 2015

Abstract The efficiency of energy consumption of a battery-powered electric vehicle (EV) is an important issue. This paper provides a comprehensive study on the effects of lateral gaps under non-lane discipline on the energy consumption for EV traffic stream by analyzing driving cycles produced by car-following models. In particular, the energy consumption model includes travel resistance power loss, motor power loss, regenerative braking power, and ancillary power loss. Then, three car-following models are implemented to evaluate the effects of lateral gaps: the FVD model with no lateral gap, the NLBCF model with one-sided lateral gap, and the TSFVD model with two-sided lateral gaps. Numerical experiments analyze three scenarios: start

process, stop process, and evolution process for FVD model, NLBCF model, and TSFVD model, respectively. Simulation results demonstrate that, although EVs under the non-lane discipline recuperate more energy during the deceleration phase, they overall consume more energy than under lane-based discipline. This study highlights that the characteristic in terms of lateral distribution of traffic flow may lead to different energy consumption in EV traffic stream. This study also provides policy insights that regularizing lane discipline contributes to the improvement in energy efficiency.

Keywords Car-following model · Electric vehicle · Energy consumption · Lateral gaps · Non-lane discipline

Yongfu Li (✉) · Li Zhang · Taixiong Zheng · Yinguo Li
Center for Automotive Electronics and Embedded System,
College of Automation, Chongqing University of Posts and
Telecommunications (CQUPT), Chongqing 400065,
People's Republic of China
e-mail: laf1212@163.com

Yongfu Li
Electronic Information and Networking Research Institute,
Chongqing University of Posts and Telecommunications
(CQUPT), Chongqing 400065, People's Republic of China

Hong Zheng · Xiaozheng He
NEXTRANS Center, Purdue University, West Lafayette,
IN 47907, USA

Srinivas Peeta
School of Civil Engineering and NEXTRANS Center,
Purdue University, West Lafayette, IN 47907, USA

1 Introduction

Compared to combustion-powered vehicles, electric vehicles (EVs) have better energy efficiency and no tailpipe emissions on the road. Many governments worldwide support the uptake of EVs to enhance energy efficiency, promote environment sustainability, and improve community livability, especially in developing countries with dense population urban areas such as China and India. According to a recent study [1], the market share of EV can comprise up to 7% of light-duty vehicles by 2020 due to the improvement of EV technologies and the increasing public acceptance.

With the increasing market share of EV, there is the research need to analyze the EV system performance in terms of energy consumption under a variety of traffic conditions. Recent studies on this topic focus on the EV's energy consumption on a road with lane discipline [2]. However, in many developing countries, lanes may not be clearly demarcated on a road though multiple vehicles can travel in parallel. Under this environment, the notion of a lane does not exist and consequently the middle of a lane is not meaningful either [3]. Hence, when an EV travels on a road without lane discipline, its speed profile and acceleration/deceleration pattern would be affected by the lateral gaps with vehicles beside it, resulting in a different energy consumption pattern. Therefore, it is worthwhile to investigate the energy consumption of EVs under non-lane-discipline environment.

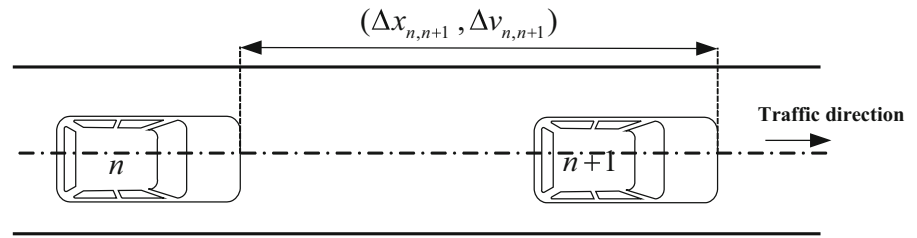
The EV energy consumption model investigated in this study relies on the drive cycles produced by microscopic traffic flow models. Microscopic traffic flow models capture the characteristics of traffic flow through the microscopic variables such as the position, velocity, and acceleration/deceleration of individual vehicle [4–9]. In 1995, Bando et al. [10] proposed an optimal velocity (OV)-based car-following model to capture the characteristics of the state evolution in transportation systems. Later, many OV-based car-following models have been developed by factoring the headway difference, velocity difference, acceleration difference, and the numbers of preceding vehicles separately or simultaneously, such as generalized force (GF) model [11], full velocity difference (FVD) model [12], multiple ahead and velocity difference (MAVD) model [13], full velocity and acceleration difference (FVAD) model [14], and multiple headway, velocity and acceleration difference (MHVAD) model [15]. Results from these car-following models show that the stop-and-go waves can be captured effectively. However, the models mentioned above are based on the assumption that vehicles follow the lane discipline and move in the middle of the lane. Besides, Jin et al. [16] proposed a non-lane-based full velocity difference car-following (NLBCF) model to analyze the impact of the lateral gap on one side on the car-following behavior. They demonstrate that considering the one-sided lateral gap can improve the stability of the traffic flow. However, there may be two lateral gaps on either side of the vehicle on a road without lane discipline. Under this scenario, the NLBCF model cannot distinguish the right-side or

the left-side lateral gaps. Recently, Li et al. [17] proposed a generalized model which considers the effects of two-sided lateral gaps of the following vehicle under non-lane-discipline environment. We label this model as the two-sided lateral gaps FVD (TSFVD) model hereafter.

In this study, the scope is restricted to battery-powered EV. One unique characteristic of EVs is that it can be equipped with the regenerative braking system (RBS), which can recuperate part of energy loss to recharge battery during the deceleration phase. Therefore, energy recuperation needs to be measured in EV energy consumption computation. In this research line, Wu et al. [17, 18] proposed an analytical model of power estimation according to the fundamental theory of vehicle dynamics and the field data. However, their model is restricted to an individual vehicle, which does not consider the impacts of surrounding vehicles in the same traffic stream. Yang et al. [2] studied the energy consumption of EVs based on a lane-based car-following model without considering lateral gaps.

The literature review heretofore illustrates that none of the previous studies analyze the energy consumption of EV traffic stream under the non-lane-discipline environment. Therefore, this study focuses on evaluating the effects of lateral gaps under non-lane-discipline environment on the energy consumption of EV traffic stream. In particular, we present an energy consumption model for EVs including the travel resistance power loss, motor power loss, regenerative braking power, and ancillary power loss. Then, this EV energy consumption model is applied to three car-following models to evaluate the impacts of lateral gaps: the FVD model without lateral gap, the NLBCF model with one-sided lateral gap, and the TSFVD model with two-sided lateral gaps. Simulation experiments are performed to investigate the velocity, acceleration/deceleration, and power consumption profiles of EV traffic stream under the scenarios of start process, stop process, and evolution process. Experimental results show that, although EVs under the non-lane discipline recuperate more energy during the deceleration phase, they overall consume more energy than lane-based discipline. This study highlights that the characteristic in terms of lateral distribution of traffic flow may lead to different energy consumption in EV traffic stream. This study also provides policy insights that regularizing lane discipline contributes to the improvement of energy efficiency.

Fig. 1 Car-following without lateral gap



The contributions of this study are summarized as follows: (1) the proposed model provides the capability to analyze the energy consumption at the system level, i.e., traffic stream, which offers a tool for planners or engineers to better assess the system performance holistically, (2) the study highlights the distinct impacts of two-sided and one-sided lateral gaps on the energy consumption of traffic stream under non-lane-based discipline, and (3) the findings of this study can also provide insights for transportation decision makers to regularize the traffic stream to follow lane discipline with respect to energy efficiency.

The rest of this paper is organized as follows. Section 2 reviews three car-following models, FVD model, NLBCF model, and TSFVD model that will be used to represent different traffic conditions in this study. Section 3 presents an energy consumption model. Section 4 conducts the numerical experiments to compare energy consumption profiles in the start process, stop process, and evolution process, respectively. The final section concludes this paper.

2 Car-following model

2.1 FVD model

For the lane-based scenario in car-following theory as shown in Fig. 1, Jiang et al. [13] proposed full velocity difference (FVD) model to capture the characteristic of vehicular traffic flow considering the velocity difference between the leading and following vehicles as follows:

$$a_n(t) = k [V(\Delta x_n(t)) - v_n(t)] + \lambda \Delta v_n(t) \quad (1)$$

where $x_n(t)$, $v_n(t)$, and $a_n(t)$ represent the position (in m), velocity (in m/s), and acceleration (in m/s^2) of the vehicle n at time t . $\Delta x_n(t) \equiv x_{n+1}(t) - x_n(t)$ and $\Delta v_n(t) \equiv v_{n+1}(t) - v_n(t)$ are the space headway difference and velocity difference between the leading vehicle

vehicle $n + 1$ and the following vehicle n . $k > 0$ and $k \in \mathbb{R}$ and $\lambda \geq 0$ and $\lambda \in \mathbb{R}$ are the sensitivity coefficients.

$V(\Delta x)$ is the optimal velocity function defined in [12]:

$$V(\Delta x) = V_1 + V_2 \tanh[C_1(\Delta x - l_c) - C_2] \quad (2)$$

where V_1 , V_2 , C_1 , C_2 are constant parameters, l_c is the vehicle length and $\tanh(\cdot)$ is the hyperbolic tangent function.

2.2 NLBCF model

Considering the scenario that there is one-sided lateral gap in the non-lane-discipline road system as shown in Fig. 2, Jin et al. [16] proposed a non-lane-based full velocity difference car-following model (NLBCF) as follows:

$$a_n(t) = k \{V[\Delta x_{n,n+1}(t), \Delta x_{n,n+2}(t)] - v_n(t)\} + \lambda G[\Delta v_{n,n+1}(t), \Delta v_{n,n+2}(t)] \quad (3)$$

where $\Delta x_{n,n+1} \equiv x_{n+1} - x_n$, $\Delta v_{n,n+1} \equiv v_{n+1} - v_n$ are the longitudinal space headway and the velocity difference between the leading vehicle $n + 1$ and the following vehicle n at time t , respectively. $\Delta x_{n,n+2} \equiv x_{n+2} - x_n$, $\Delta v_{n,n+2} \equiv v_{n+2} - v_n$ are the longitudinal space headway and the velocity difference between the leading vehicle $n + 2$ and the following vehicle n at time t , respectively.

The functions $V[\Delta x_{n,n+1}(t), \Delta x_{n,n+2}(t)]$ and $G[\Delta v_{n,n+1}(t), \Delta v_{n,n+2}(t)]$ are represented as follows [16]:

$$\begin{aligned} & V[\Delta x_{n,n+1}(t), \Delta x_{n,n+2}(t)] \\ &= V[(1 - p_n)\Delta x_{n,n+1}(t) + p_n\Delta x_{n,n+2}(t)] \end{aligned} \quad (4)$$

$$\begin{aligned} & G[\Delta v_{n,n+1}(t), \Delta v_{n,n+2}(t)] \\ &= (1 - p_n)\Delta v_{n,n+1}(t) + p_n\Delta v_{n,n+2}(t) \end{aligned} \quad (5)$$

where $p_n \equiv Lg_{n,n+1}/Lg_{\max}$ is the effect parameter of lateral gap. $Lg_{n,n+1}$ is the lateral gap between vehicle $n + 1$ and vehicle n , and Lg_{\max} is the maximal lateral gap.

Fig. 2 Car-following with one-sided lateral gap

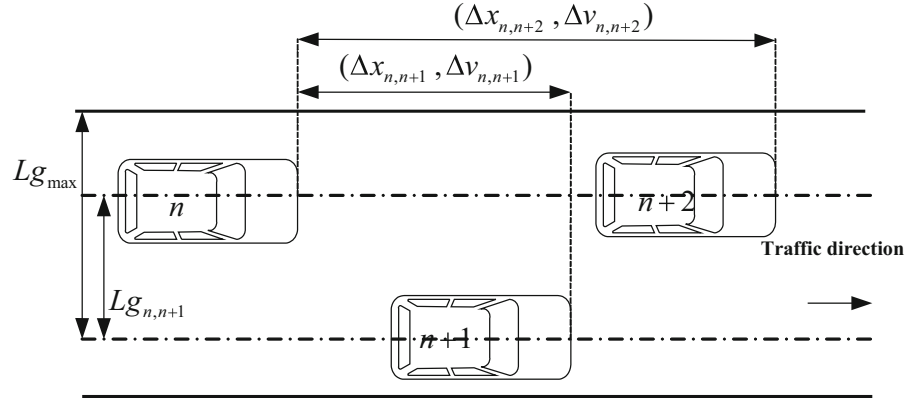
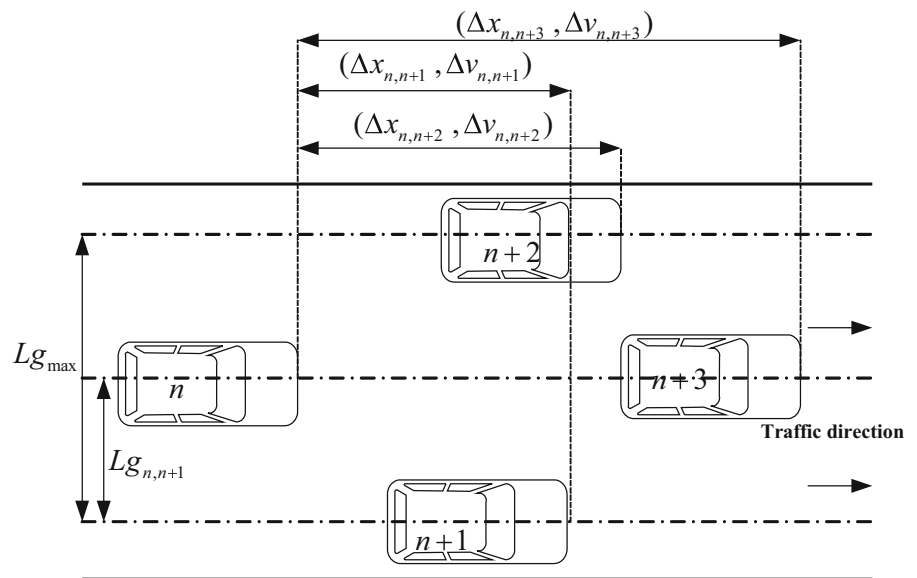


Fig. 3 Car-following with two-sided lateral gaps



2.3 TSFVD model

Considering the scenario that there are two-sided lateral gaps in the non-lane-discipline road system as shown in Fig. 3, Li et al. [17] proposed a non-lane-discipline-based FVD car-following model considering the effects of two-sided lateral gaps (TSFVD) as follows:

$$\begin{aligned} a_n(t) = & k \left\{ V [\Delta x_{n,n+1}(t), \Delta x_{n,n+2}(t), \Delta x_{n,n+3}(t)] \right. \\ & - v_n(t) \} \\ & + \lambda G [\Delta v_{n,n+1}(t), \Delta v_{n,n+2}(t), \Delta v_{n,n+3}(t)] \end{aligned} \quad (6)$$

where $\Delta x_{n,n+3} \equiv x_{n+3} - x_n$, $\Delta v_{n,n+3} \equiv v_{n+3} - v_n$ are the longitudinal space headway and the velocity

difference between the leading vehicle $n+3$ and the following vehicle n at time t , respectively.

The functions $V[\Delta x_{n,n+1}(t), \Delta x_{n,n+2}(t), \Delta x_{n,n+3}(t)]$ and $G[\Delta v_{n,n+1}(t), \Delta v_{n,n+2}(t), \Delta v_{n,n+3}(t)]$ are represented as follows [17]:

Case (i): $Lg_{n,n+1} \in [0, 0.5Lg_{\max}]$

$$\begin{aligned} V [\Delta x_{n,n+1}(t), \Delta x_{n,n+2}(t), \Delta x_{n,n+3}(t)] \\ = V [(1 - 2p_n)\Delta x_{n,n+1}(t) + 2p_n\Delta x_{n,n+3}(t)] \end{aligned} \quad (7)$$

$$\begin{aligned} G [\Delta v_{n,n+1}(t), \Delta v_{n,n+2}(t), \Delta v_{n,n+3}(t)] \\ = (1 - 2p_n)\Delta v_{n,n+1}(t) + 2p_n\Delta v_{n,n+3}(t) \end{aligned} \quad (8)$$

Case (ii): $Lg_{n,n+1} \in [0.5Lg_{\max}, Lg_{\max}]$

$$\begin{aligned} V [\Delta x_{n,n+1}(t), \Delta x_{n,n+2}(t), \Delta x_{n,n+3}(t)] \\ = V [(2p_n - 1)\Delta x_{n,n+2}(t) + 2(1 - p_n)\Delta x_{n,n+3}(t)] \end{aligned} \quad (9)$$

$$\begin{aligned} G & [\Delta v_{n,n+1}(t), \Delta v_{n,n+2}(t), \Delta v_{n,n+3}(t)] \\ & = (2p_n - 1)\Delta v_{n,n+2}(t) + 2(1 - p_n)\Delta v_{n,n+3}(t) \end{aligned} \quad (10)$$

3 Energy consumption model

In this study, we present an energy consumption model including the travel resistance power loss, motor power loss, regenerative braking power, and ancillary power loss.

3.1 Travel resistance power loss P_t

According to basic physics, the required tractive effort for an EV driving on certain conditions is determined by four major resistances as described by the following equation:

$$F = F_m + F_a + F_r + F_t \quad (11)$$

where F is tractive effort (in N); F_m , F_a , F_r , F_t are the forces associated with the acceleration of EV, aerodynamic drag, rolling resistance and wheel/axle bearing friction, respectively. And they are given by [18–20]:

$$\begin{cases} F_m = ma \\ F_a = \alpha v^2 = 0.5\rho C_D A_f v^2 \\ F_r = f_r mg \\ F_t = \frac{bv}{R_t} \end{cases} \quad (12)$$

where m is the vehicle mass (in kg); a is acceleration (in m/s^2); v is the vehicle velocity (in m/s); α is aerodynamic resistance constant determined by air density ρ (in kg/m^3), frontal area of the vehicle A_f (in m^2) and coefficient of drag C_D . f_r is rolling resistance constant and g is gravity acceleration ($g = 9.81 \text{ m/s}^2$); b is the bearings damping coefficient and R_t is an effective EV tire radius.

Hence, the travel resistance power loss P_t for EV with the velocity v can be measured using the following equation:

$$P_t = \left(\alpha v^2 + f_r mg + \frac{bv}{R_t} \right) \cdot v \quad (13)$$

3.2 Motor power loss P_m

According to the electricity theory, the power losses could be described as a product of the square of the

current (I) and the resistance of the conductor (r). Therefore, the motor power loss is given by:

$$P_m = I^2 r \quad (14)$$

On the other hand, the tractive effort F is generated by the torque of the motor, which can be simplified as a product of the armature constant (K_a), magnetic flux (ϕ_d), and current (I):

$$F = \frac{J}{R_t} = \frac{K_a \cdot \phi_d \cdot I}{R_t} \quad (15)$$

where J (in Nm) is the torque; K_a is the armature constant; ϕ_d (in webe) is the magnetic flux; and I (in A) is the current.

For simplicity, by defining $K = K_a \cdot \phi_d$ and we obtain:

$$F = \frac{K \cdot I}{R_t} \quad (16)$$

Based on Eqs. (11), (14), and (16), the motor power loss can be rewritten as [18,19]:

$$P_m = \frac{r \cdot R_t^2}{K^2} \left(ma + \alpha v^2 + f_r mg + \frac{bv}{R_t} \right)^2 \quad (17)$$

3.3 Regenerative braking power P_g

Compared to internal combustion engine vehicles, one of the most advanced features of an EV is its ability to capture and store energy through the RBS, which uses the electric motor to recharge the battery by applying negative torque to the drive wheels and converting kinetic energy to electrical energy. The initial kinetic energy is transformed into electrical energy by the generator and is then converted into chemical energy by the battery [20]. The regenerative braking power can be described as follows [18,19]:

$$P_g = \eta \cdot mav \quad (18)$$

where η is the efficiency of the generator.

3.4 Ancillary power loss P_a

Part of the electricity energy of EV may be consumed by some vehicle ancillaries. Examples are user-related systems such as air conditioner, external lights, and audio, as well as systems necessary to regulate battery temperature. Thus, the ancillary power loss is given by [20]:

$$P_a = P_{ac} + P_{bm} + P_{el} + P_{au} \quad (19)$$

Table 1 The values of parameters in the car-following models

Parameter	Value	Unit
k	0.85	s^{-1}
λ	0.5	s^{-1}
v_{\max}	2.0	m/s
h_c	2.0	m
N	11	—
L	500	m
V_1	6.75	m/s
V_2	7.91	m/s
C_1	0.13	m^{-1}
C_2	1.57	—
l_c	5.0	m

where P_{ac} , P_{bm} , P_{el} , P_{au} are energy consumptions of air conditioner, battery management, external lights, and audio, respectively. Note that all of the above ancillaries energy consumption are independent of velocity.

Based on the foregoing discussion in Sects. 3.1–3.4, an EV's instantaneous power can be measured by:

$$P = P_t + P_m + P_g + P_a \quad (20)$$

4 Numerical experiments

To perform the simulations, the values of parameters used in the car-following and the energy consumption models are summarized in Table 1 [10–17] and Table 2 [2, 18, 19], respectively. Moreover, in order to analyze the effect of lateral gaps on the energy consumption of EV traffic stream, we compare simulation results based on FVD model without lateral gap, NLBCF model with one-sided lateral gap, and TSFVD model with two-sided lateral gaps under the start, stop, and evolution processes, respectively. The initial condition is as follows. Eleven EVs are distributed in a road with the equal space headway of 7.4 m. The 11th vehicle is the leading one.

4.1 Start process

The start process is set up as follows. Initially, the traffic signal is red, and all EVs are waiting behind the signal with the uniform space headway. At time $t = 0$ s, the signal changes to green and the EVs start to move. The

Table 2 The values of parameters in the energy consumption models

Parameter	Value	Unit
m	1500	kg
f_r	0.015	—
C_D	0.3	—
A_f	1.8	m^2
ρ	1.2	kg/m^3
r	0.11	Ω
η	0.3	—
g	9.81	m/s^2
R_t	0.3	m
b	1.0	m
P_a	2.0	kW

leading vehicle starts to accelerate until it reaches the optimal speed. The other vehicles follow the leading vehicle to accelerate. Eventually, all vehicles travel at the same optimal velocity. For comparison, the velocity, acceleration, and power consumption profiles of FVD model, NLBCF model, and TSFVD model are illustrated in Figs. 4, 5 and 6, respectively.

Figure 4 demonstrates that TSFVD model with two-sided lateral gaps is the most responsive, followed by NLBCF model with one-sided lateral gap, then FVD model without lateral gap. It indicates that the lateral gap can increase the responsiveness of velocity. Here, the responsiveness of EV traffic stream means that vehicles react to accelerate/decelerate quickly. Figure 5 demonstrates that the magnitude of acceleration for FVD model is the largest, followed by NLBCF model, then TSFVD model. Specifically, the maximum acceleration in TSFVD model is about 3 m/s^2 , which is less than that of FVD model and BLBCF model. It shows that lateral gaps reduce the magnitude of acceleration. On the other hand, vehicles in FVD model and NLBCF model start to accelerate one by one with a transition period. In contrast, vehicles in TSFVD model start to accelerate in a short time. Based on Eqs. (13), (17), (18), and (20), the power consumption is relevant to the velocity and acceleration of EVs. Figure 6 shows that there are three stages in the power consumption profile for all models. In the first stage, the power consumption increases sharply due to the increase in velocity and acceleration. In the second stage, the power consumption decreases

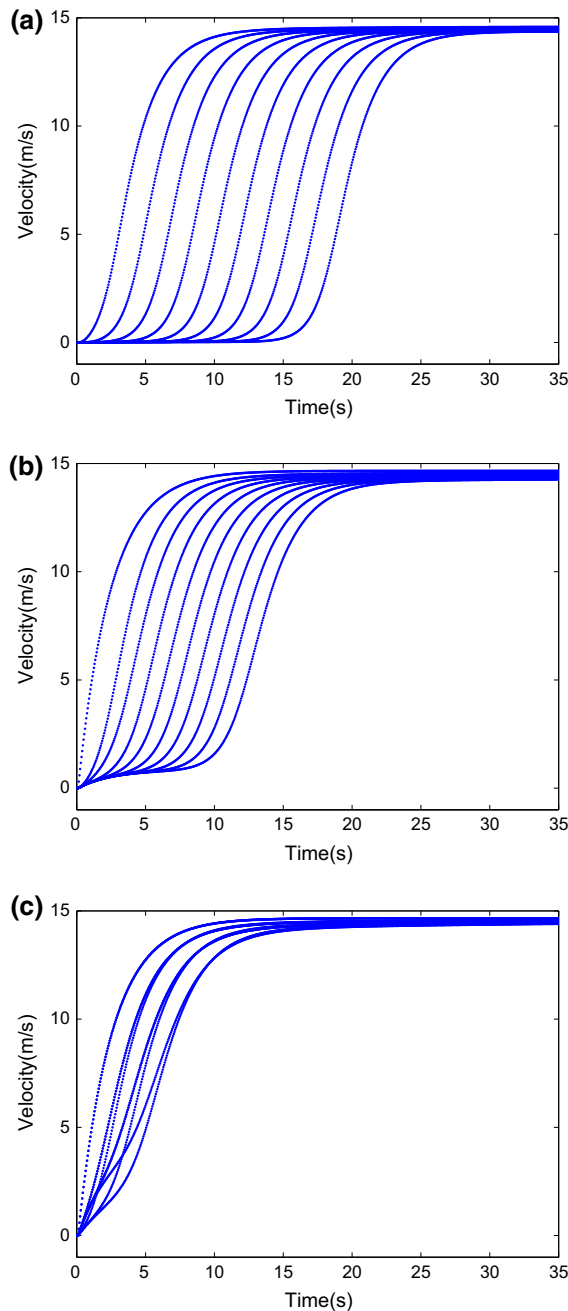


Fig. 4 The velocity profile of EV traffic stream starting from a green traffic signal: **a** FVD model; **b** NLBCF model ($p_n = 0.3$); **c** TSFVD model ($p_n = 0.7$)

because the acceleration is reduced although the velocity keeps increasing. In the third stage, acceleration becomes zero, and the power consumption becomes stable maintaining the ancillary power usage. Table 3

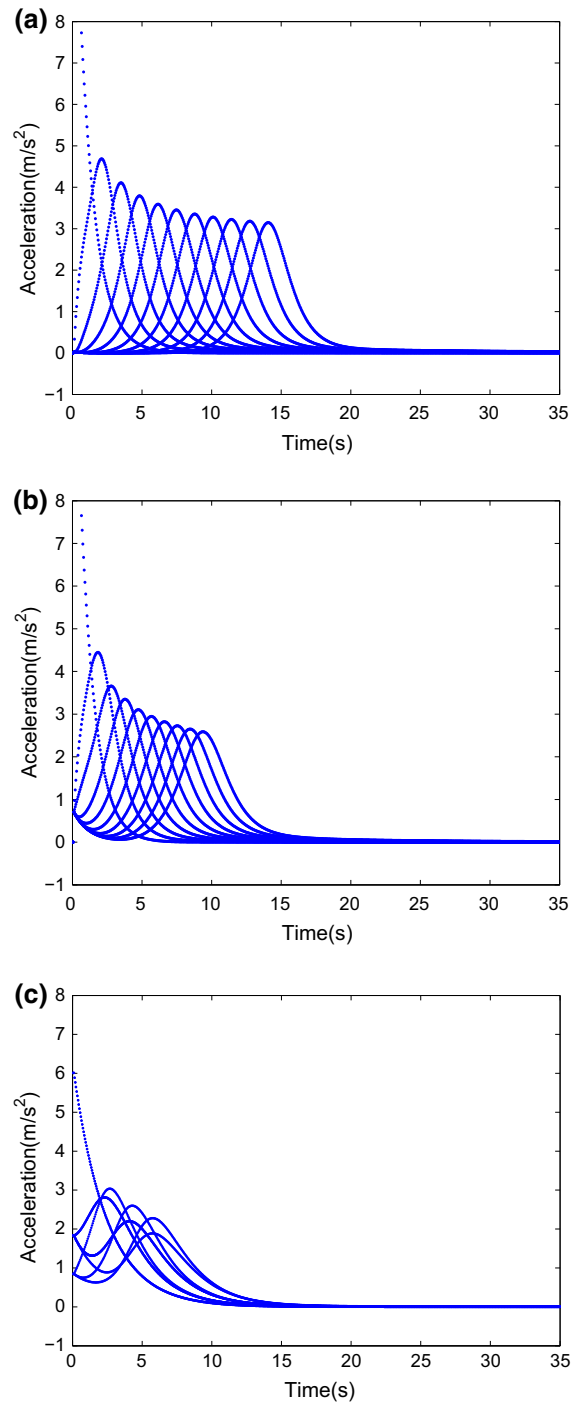


Fig. 5 The acceleration profile of EV traffic stream starting from a green traffic signal: **a** FVD model; **b** NLBCF model ($p_n = 0.3$); **c** TSFVD model ($p_n = 0.7$)

demonstrates that vehicles in FVD model consume the least energy, and vehicles in TSFVD model consume the most energy. This is because vehicles in TSFVD

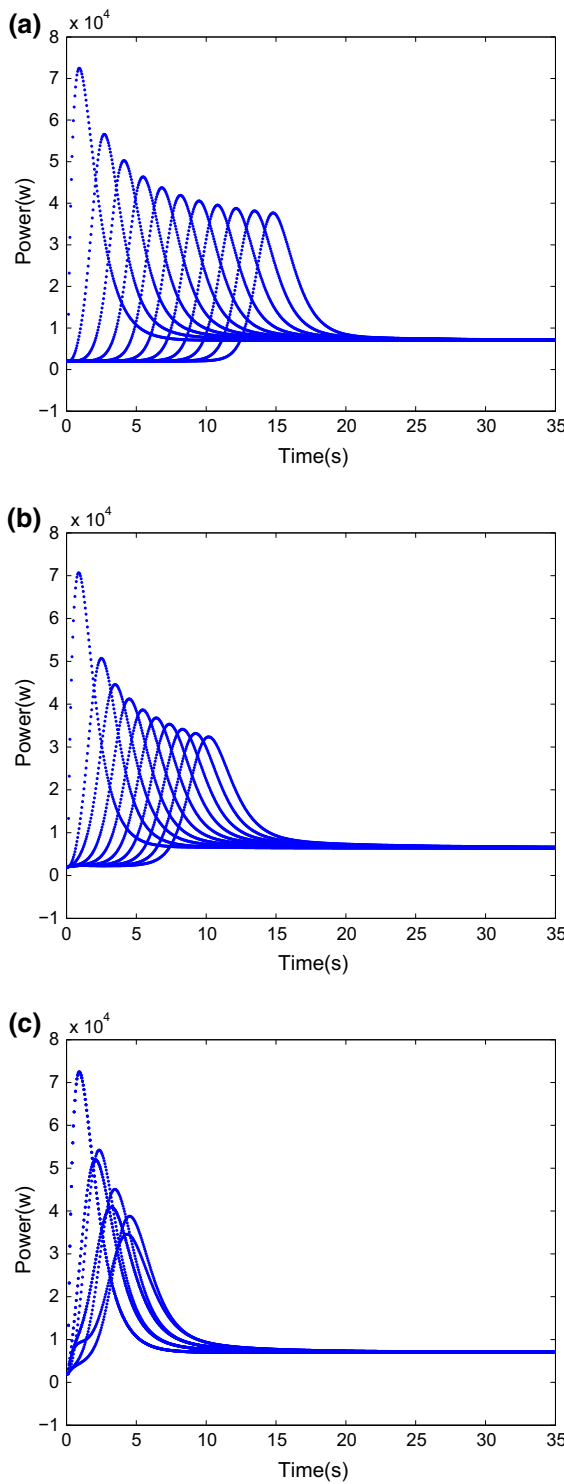


Fig. 6 The power consumption profile of EV traffic stream starting from a green traffic signal: **a** FVD model; **b** NLBCF model ($p_n = 0.3$); **c** TSFVD model ($p_n = 0.7$)

Table 3 The total energy of EV traffic stream

Model	FVD	NLBCF	TSFVD
In the start process (10^6 J)	3.6258	4.1743	4.4702
In the stop process (10^6 J)	3.2113	3.9070	4.0539
In the evolution process (10^6 J)	2.8361	2.8422	3.0849

model with two-sided lateral gaps accelerate earlier and thus travel longer distance and consume more energy than those in FVD model and NLBCF model. Therefore, considering lateral gaps under non-lane discipline increases the energy consumption in the start process. In addition, Fig. 6 shows that the power consumption starts from a nonzero value, this is because we consider the ancillary power loss which is a constant value in the energy consumption model.

4.2 Stop process

The stop process is set up as follows. Initially, the traffic signal is green and all EVs are traveling at the same constant velocity. At time $t = 0$ s, the signal changes to red and EVs begin to slow down. The leading vehicle begins to decelerate until it reaches a full stop. The other vehicles follow the leading vehicle to decelerate. Finally, all vehicles fully stop behind the signal. For comparison, the velocity, deceleration, and power consumption profiles of FVD model, NLBCF model, and TSFVD model are illustrated in Figs. 7, 8, and 9, respectively.

Figure 7 demonstrates that TSFVD model is the most responsive, followed by NLBCF model, then FVD model. This pattern is the same with the start process, which indicates the lateral gap can increase the responsiveness of velocity. Figure 8 demonstrates that the magnitude of deceleration for TSFVD model is the largest, followed by NLBCF model, then FVD model. This pattern is opposite to the start process. Specifically, the maximum deceleration in TSFVD model exceeds -4 m/s^2 , which is more than that of FVD model and NLBCF model. It implies that lateral gaps increase the magnitude of deceleration. In Fig. 9, the value of power consumption is negative, which implies the battery is recharged through the RBS during the deceleration phase. There are also three stages in the power con-

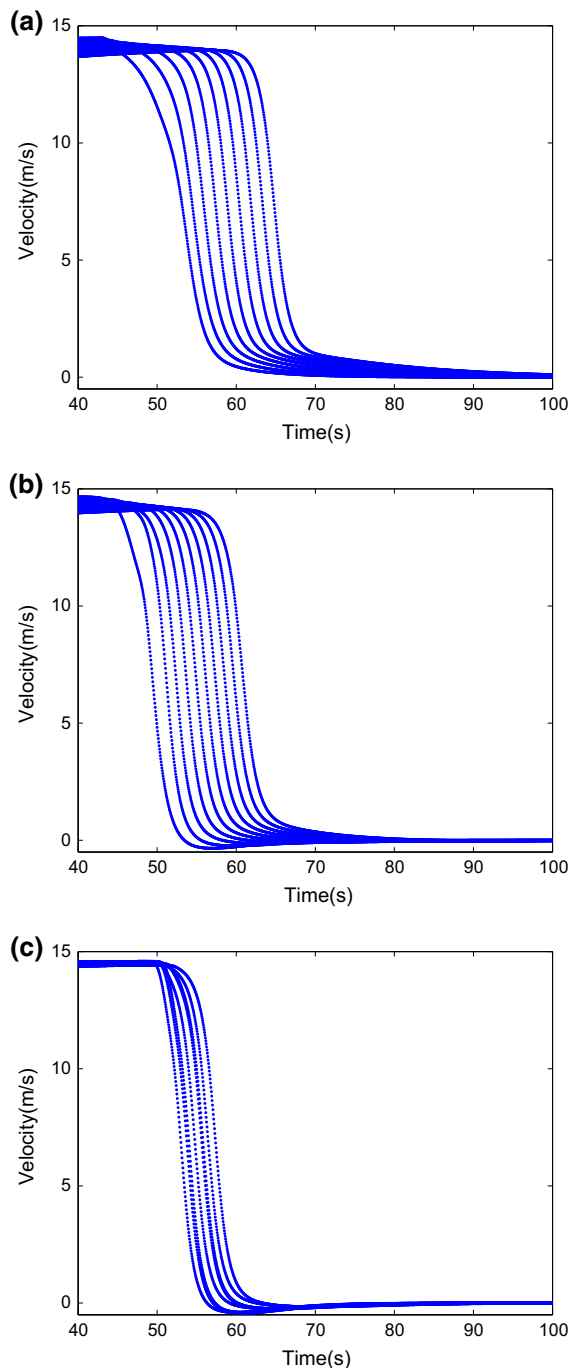


Fig. 7 The velocity profile of EV traffic stream stopping at a red traffic signal: **a** FVD model; **b** NLBCF model ($p_n = 0.3$); **c** TSFVD model ($p_n = 0.7$)

sumption profile. In the first stage, the power consumption decreases sharply due to the decrease in velocity and deceleration. In the second stage, the power con-

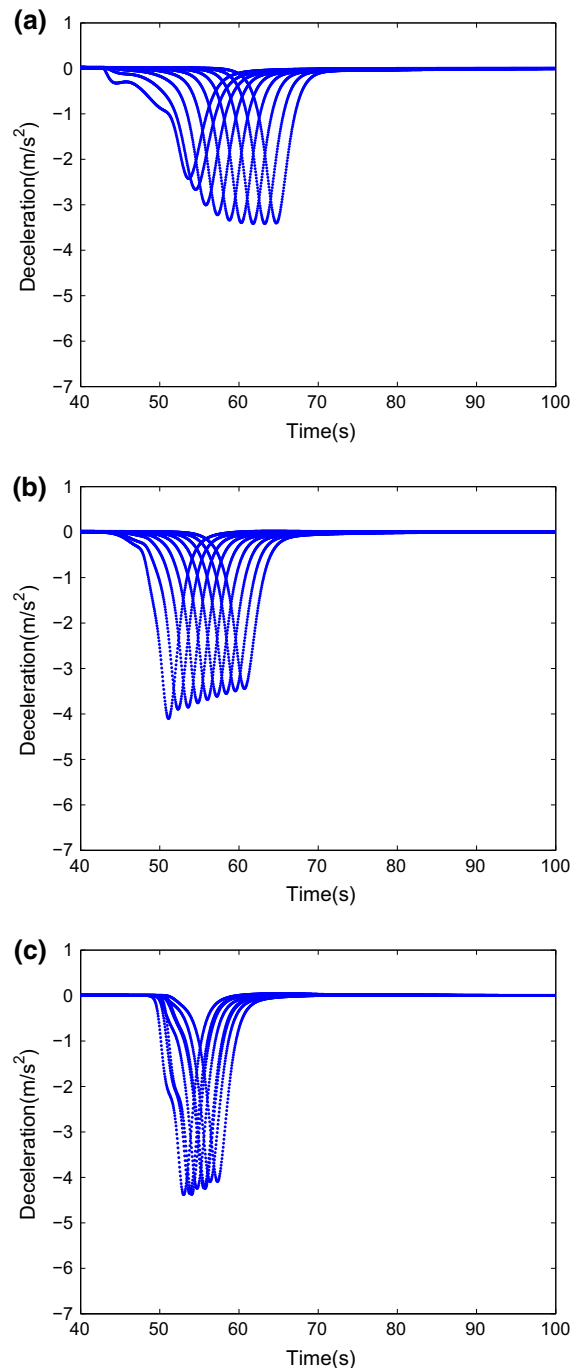


Fig. 8 The deceleration profile of EV traffic stream stopping at a red traffic signal: **a** FVD model; **b** NLBCF model ($p_n = 0.3$); **c** TSFVD model ($p_n = 0.7$)

sumption increases. In the third stage, the velocity and deceleration are zero, the power consumption becomes stable maintaining the ancillary power usage. Table 3

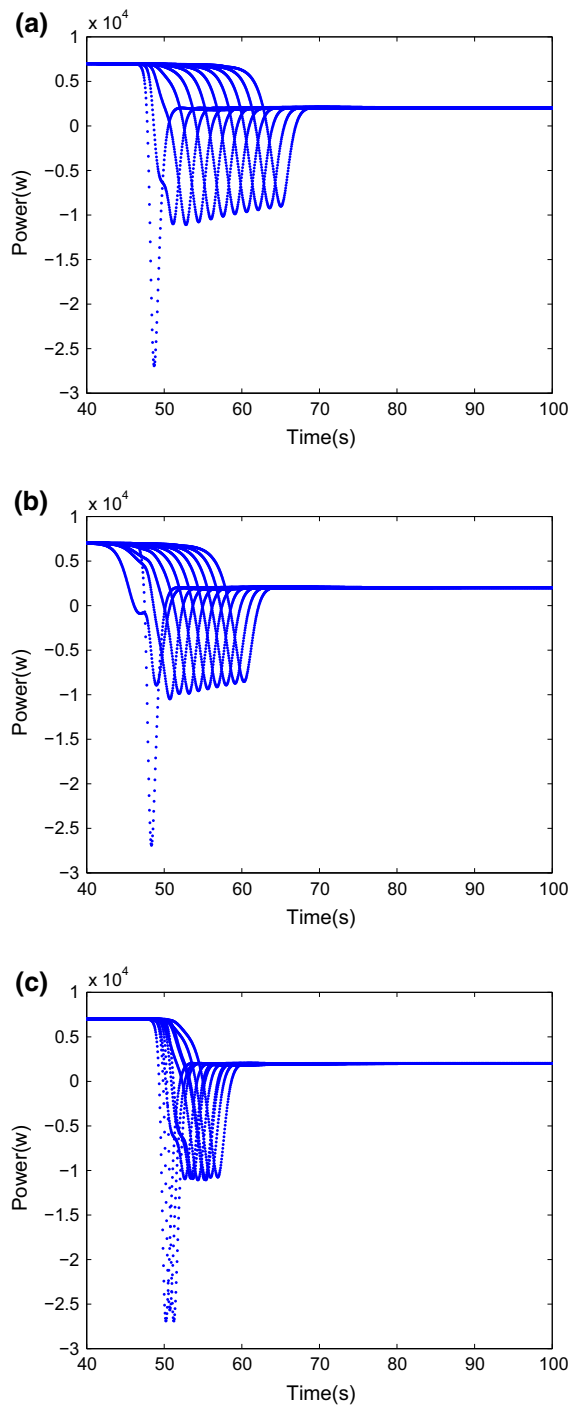


Fig. 9 The power consumption profile of EV traffic stream stopping at a red traffic signal: **a** FVD model; **b** NLBCF model ($p_n = 0.3$); **c** TSFVD model ($p_n = 0.7$)

indicates that vehicles in TSFVD model recuperates the most energy, and vehicles in FVD model recuperates the least energy.

4.3 Evolution process

In this section, the evolution process combining the start and stop processes is discussed. The leading vehicle first starts to move from the zero velocity, and then decelerates to a full stop. The other vehicles follow the leading vehicle according to FVD model, NLBCF model, and TSFVD model, respectively. For comparison, Figs. 10, 11, and 12 show the velocity, acceleration, and power consumption profiles.

Figure 10 demonstrates that TSFVD model is the most responsive, followed by NLBCF model, then FVD model, which is consistent with the observations in the start and stop processes. Figure 11 demonstrates that vehicles in FVD model and NLBCF model start to accelerate/decelerate one by one with a transition period. Vehicles in TSFVD model, however, accelerate/decelerate more quickly. In Fig. 12, the energy consumption can be divided into two parts in general: (1) power consumption during the acceleration phase and (2) power recuperation during the deceleration phase. Overall, vehicles in FVD model consume the least energy in the first part, and recuperate the least energy in the second part. In contrast, vehicles in TSFVD model consume the most energy in the first part, and recuperate the most energy in the second part.

The total power consumption profile of FVD model, NLBCF model, and TSFVD model in the evolution process is shown in Fig. 13. Figure 13 demonstrates that considering lateral gaps under non-lane-discipline environment will consume more of total energy. To verify this point, the values of total energy consumption of the three different car-following models are shown in Table 3. Table 3 shows the total energy consumption of FVD model, NLBCF model, and TSFVD model are 2.8361×10^6 J, 2.8422×10^6 J, and 3.0849×10^6 J, respectively. Note that we give the total energy consumption of the 8 following EVs in the traffic stream for comparison, because the 9th, 10th, and the 11th vehicles are the boundary in the TSFVD model.

Based on Sects. 4.1–4.3 discussed above, the main findings can be summarized as follows: (1) Considering the effects of lateral gaps, the EV traffic stream consumes more energy in acceleration phase and recuperates more energy in deceleration phase than the case of without lateral gap. This is because vehicles in the car-following model under the non-lane-based discipline react more quickly than the lane-based discipline. It can represent the scenario that drivers operate their vehicles

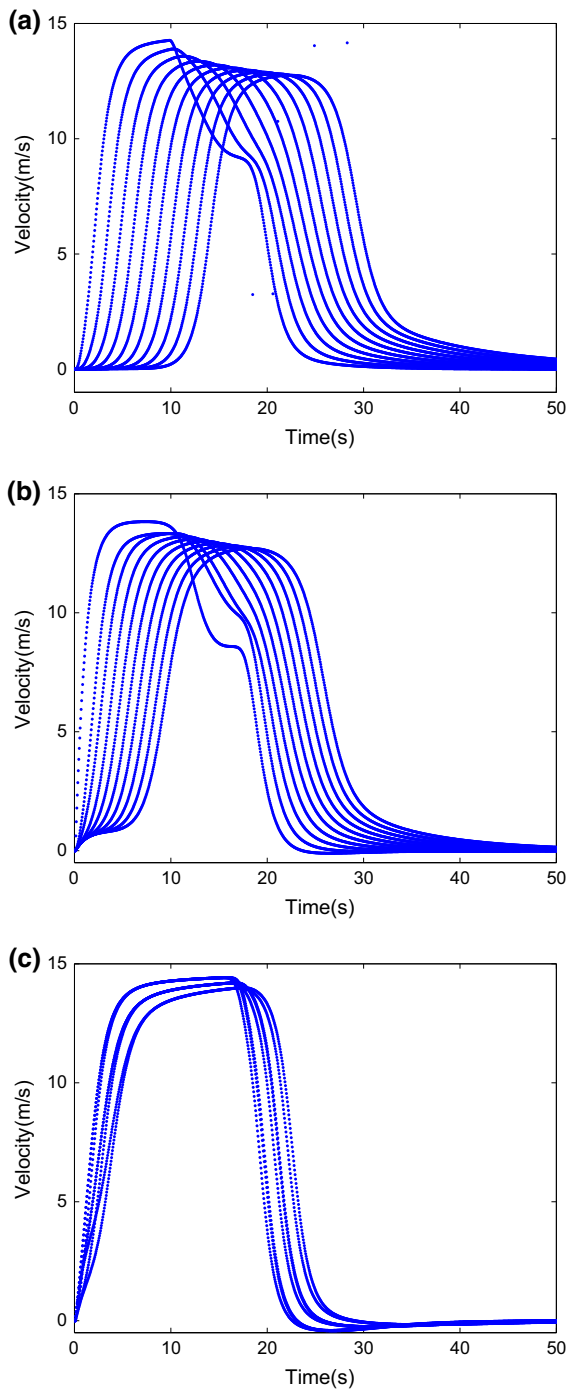


Fig. 10 The velocity profile of EV traffic stream evolution: **a** FVD model; **b** NLBCF model ($p_n = 0.3$); **c** TSFVD model ($p_n = 0.7$)

more aggressively on a road without lane-discipline. (2) Considering the effects of lateral gaps, the EV traffic stream is more responsive to accelerate /decelerate.

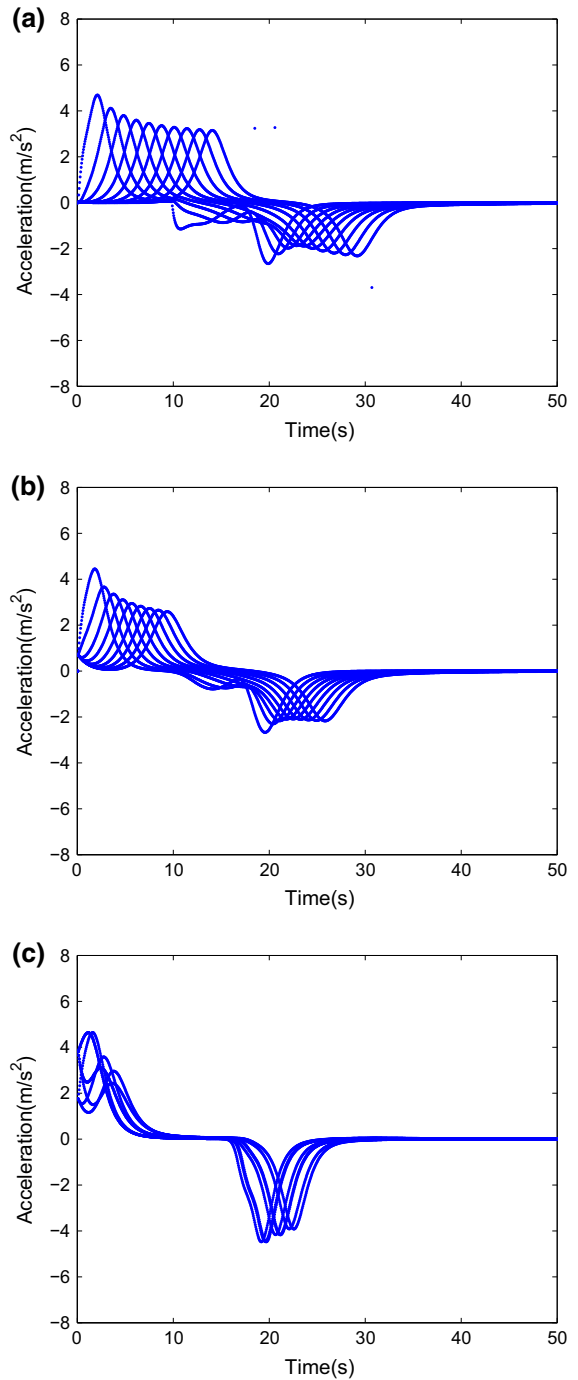


Fig. 11 The acceleration profile of EV traffic stream evolution: **a** FVD model; **b** NLBCF model ($p_n = 0.3$); **c** TSFVD model ($p_n = 0.7$)

(3) The influence of two-sided lateral gaps is greater than that of the one-sided lateral gap in the non-lane-discipline road system.

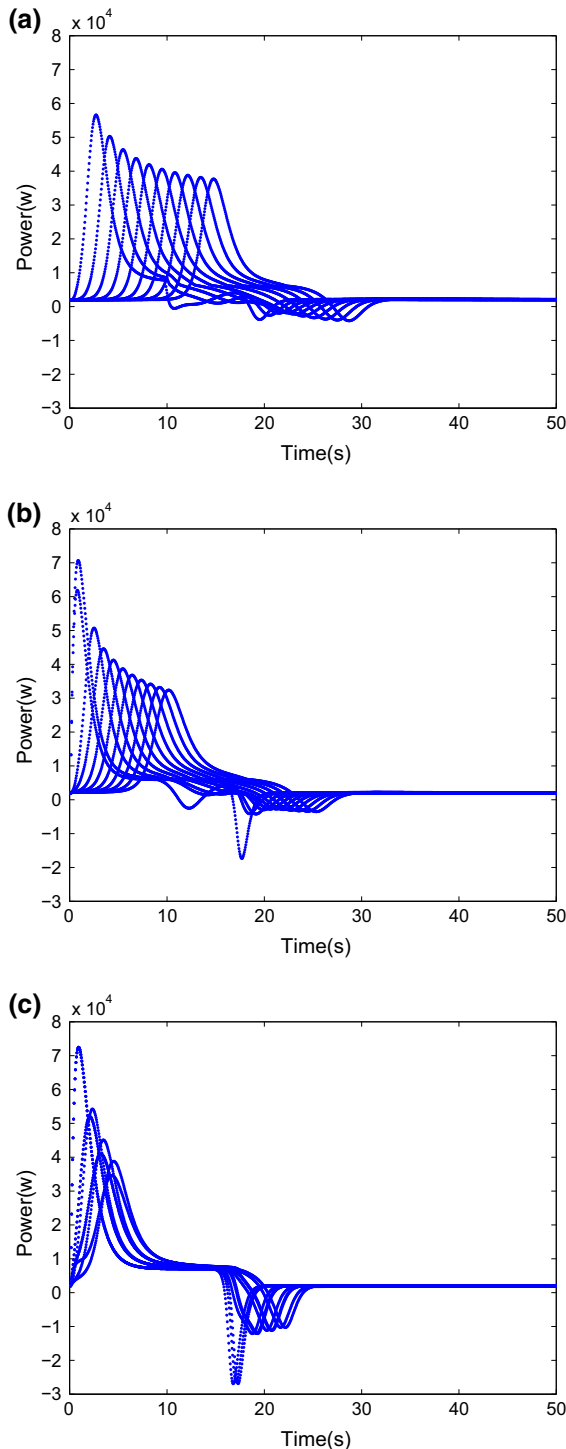


Fig. 12 The power consumption profile of EV traffic stream evolution: **a** FVD model; **b** NLBCF model ($p_n = 0.3$); **c** TSFVD model ($p_n = 0.7$)

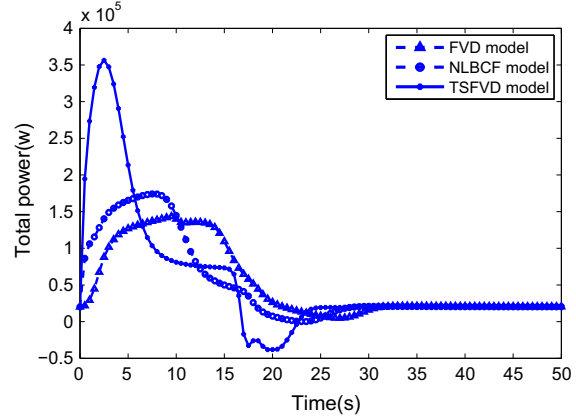


Fig. 13 The total power consumption profile of EV traffic stream evolution

5 Conclusions

This study analyzes the effects of lateral gaps on the energy consumption of EV traffic stream based on car-following models. To evaluate the effects of lateral gaps, three car-following models, FVD model without lateral gap, NLBCF model with one-sided lateral gap, and TSFVD model with two-sided lateral gaps, are used for comparison. An energy consumption model consisting of the travel resistance power loss, motor power loss, regenerative braking power, and ancillary power loss is adopted to study the energy consumption. Numerical experiments are performed to illustrate the effects of lateral gaps on the velocity, acceleration, and energy consumption profiles in the start, stop, and evolution processes.

Simulation results show that, under a road system without lane discipline, the EV traffic stream consumes more energy although it can recuperate more energy back to the battery. The reason is mainly because the EVs are more responsive, resulting in an earlier acceleration representing the aggressive driving behavior under non-lane-discipline environment. It highlights the policy need to regularize traffic stream to follow the lane discipline, from the perspective of improving energy efficiency. In addition, the findings of this study provide insights into analyzing the formation of EV platoon in the non-lane-discipline road system, considering the capacity improvement and energy consumption reduction.

Acknowledgments Thanks go to the support from the project by the National Natural Science Foundation of China (Grant No. 61304197), the Scientific and Technological Talents of Chongqing (Grant No. cstc 2014kjrc-qnrc30002), the Natural Science Funds of Education Committee of Chongqing (Grant No. KJ130506), Natural Science Funds of CQUPT (Grant No. A2012-78), Doctoral Start-up funds of CQUPT (Grant No. A2012-26), and the U.S. Department of Transportation through the NEXTRANS Center, the USDOT Region 5 University Transportation Center.

References

1. Hurst, D., Gartner, J.: Executive summary: electric vehicle market forecasts; global forecasts for light duty hybrid, plug-in hybrid, and battery electric vehicles 2013–2020. Electric Vehicle Market Forecasts (2013)
2. Yang, S., Deng, C., Tang, T., Qian, Y.: Electric vehicle's energy consumption of car-following models. *Nonlinear Dyn.* **71**, 323–329 (2013)
3. Chandra, S., Kumar, U.: Effect of lane width on capacity under mixed traffic conditions in India. *J. Transp. Eng.* **129**(2), 155–160 (2003)
4. Ossen, S., Hoogendoorn, S.P.: Heterogeneity in car-following behavior: theory and empirics. *Transp. Res. Part C Emerg. Technol.* **19**(2), 182–195 (2011)
5. Wilson, R.E., Ward, J.A.: Car-following models: fifty years of linear stability analysis—a mathematical perspective. *Transp. Plan Technol.* **34**(1), 3–18 (2011)
6. Li, Y., Sun, D.: Microscopic car-following model for the traffic flow: the state of the art. *J. Control Theory Appl.* **10**(2), 133–143 (2012)
7. Tang, T., Wang, Y., Yang, X., Wu, Y.: A new car-following model accounting for varying road condition. *Nonlinear Dyn.* **70**(2), 1397–1405 (2012)
8. Li, Y., Zhu, H., Cen, M., Li, Y., Li, R., Sun, D.: On the stability analysis of microscopic traffic car-following model: a case study. *Nonlinear Dyn.* **74**(1–2), 335–343 (2013)
9. Tang, T., Shi, W., Shang, H., Wang, Y.: A new car-following model with consideration of inter-vehicle communication. *Nonlinear Dyn.* **76**(4), 2017–2023 (2014)
10. Bando, M., Hasebe, K., Nakayama, A., Shibata, A., Sugiyama, Y.: Dynamics model of traffic congestion and numerical simulation. *Phys. Rev. E* **1**(51), 1035–1042 (1995)
11. Helbing, D., Tilch, B.: Generalized force model of traffic dynamics. *Phys. Rev. E* **58**, 133–138 (1998)
12. Jiang, R., Wu, Q.S., Zhu, Z.J.: Full velocity difference model for a car-following theory. *Phys. Rev. E* **64**, 017101–017105 (2001)
13. Sun, D., Li, Y., Tian, C.: Car-following model based on the information of multiple ahead & velocity difference. *Syst. Eng. Theory Pract.* **30**(7), 1326–1332 (2010)
14. Zhao, X., Gao, Z.: A new car-following model: full velocity and acceleration difference model. *Eur. Phys. J. B* **47**(1), 145–150 (2005)
15. Li, Y., Sun, D., Liu, W., Zhang, M., Zhao, M., Liao, X., Tang, L.: Modeling and simulation for microscopic traffic flow based on multiple headway, velocity and acceleration difference. *Nonlinear Dyn.* **66**(1–2), 15–28 (2011)
16. Jin, S., Wang, D., Tao, P., Li, P.: Non-lane-based full velocity difference car following model. *Phys. A Stat. Mech. Appl.* **389**(21), 4654–4662 (2010)
17. Li, Y., Zhang, L., Peeta, S., Pan, H., Zheng, T., Li, Y., He, X.: Non-lane-discipline-based car-following model considering the effects of two-sided lateral gaps. *Nonlinear Dyn.* **80**(1–2), 227–238 (2015)
18. Wu, X., Freese, D., Cabrera, A., Kitch, W.A.: Electric vehicles' energy consumption measurement and estimation. *Transp. Res. D* **34**, 52–67 (2015)
19. Wu, X., He, X., Yu, G., Harmandayan, A., Wang, Y.: Energy-optimal speed control for electric vehicles on signalized arterials. *IEEE Trans. Intell. Transp. Syst.* (2015). doi:[10.1109/TITS.2015.2422778](https://doi.org/10.1109/TITS.2015.2422778)
20. Van Haaren, R.: Assessment of electric cars range requirements and usage patterns based on driving behavior recorded in the National Household Travel Survey of 2009. Earth and Environmental Engineering Department, Columbia University, Fu Foundation School of Engineering and Applied Science, New York (2011)